Radio Science, Volume 10, Number 2, pages 139–147, February 1975

Microwave scattering and the straining of wind-generated waves

W. C. Keller and J. W. Wright

Ocean Sciences Division, Naval Research Laboratory, Washington, DC 20375

(Received July 3, 1974.)

The modulation in backscattered power from wind-generated waves due to the presence of a 0.575-Hz plunger-generated wave has been measured in a wave tank as a function of air friction velocity and plunger wave amplitude. The measurements were made at 9.375 GHz, a depression angle of 45° and vertical polarization. The straining of the wind waves is treated by a first-order perturbation of the Boltzmann transport equation and the scattering is calculated from a simple application of composite surface scattering theory utilizing first-order Bragg scattering. The theory predicts a characteristic relaxation behavior for the wind-speed dependence of the components of the modulation amplitude in phase and out of phase with the horizontal component of orbital velocity of the plunger wave. This relaxation behavior is closely followed by the observed modulation amplitudes for air friction velocities less than about 40 cm sec^{-1}, i.e., winds less than about 7 m sec^{-1}.

1. INTRODUCTION

Visual observation shows us that most wind-generated wave systems are two, or more, scale processes. That is, in a simple case, say, the wave system consists of a dominant wave which grows slowly in wavelength, speed, and amplitude with increasing wind speed and/or fetch and a small-scale structure which exists in some sort of steady state brought about by the wind, dissipation forces, and interaction with the dominant waves themselves. It is well established [*Wright*, 1968; *Guinard and Daley*, 1970; *Wright and Keller*, 1971] that microwave radars sense these small-scale waves when the scattering direction is away from the specular. Now, suppose a microwave beam illuminates an area of linear dimensions small compared to the dominant wavelength of a two-scale wave system (Figure 1). The power received at the antenna will vary as the large wave sweeps through the illuminated area for at least two reasons. Firstly, the scattering cross section per unit area, σ^0, depends, in general, on the local angle of incidence (or its complement, the local depression angle θ', Figure 1). Since the small waves are tilted by the large wave this angle depends on position with respect to the large wave. Secondly, the amplitude of the small waves is modified by a variety of hydrodynamic interactions with the large wave. The local scattering cross section depends on this amplitude. In fact, in first-order scattering theory, the cross section and *power spectral* amplitude are proportional [*Wright*, 1968].

It is precisely the modulation of scattering by the larger waves which makes these larger waves detectable by incoherent microwave radar. This modulation may also be of oceanographic importance for it is conjectured that much of the wind stress is transmitted from atmosphere to ocean by means of the momentum of the small waves. If the small wave amplitude is modulated, then so is the stress, and a modulated stress, if of the proper phase, will result in large wave growth. Thus the small wave structure may be important in the process of large wave generation as well as the generation of mean oceanic currents.

In this paper we report on some two-scale scattering measurements made in the laboratory. The wave tank facility, instrumentation, and measurement technique are described in section 2. The large-scale waves used in the experiments were periodic, plunger-generated waves with little cross-tank variation, and a straightforward composite surface scattering calculation, given in section 3, is used to describe the effect of variation of local angle of incidence (tilting). The straining of wind-generated waves is treated by a first-order perturbation of the Boltzmann transport equation in section 4. The relaxation time theory obtained in section 4 is compared with the experimental scattering results in section 5. It is

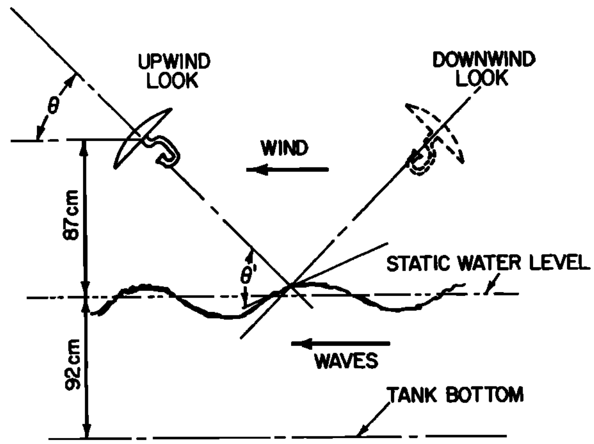

Fig. 1. Schematic diagram of the experiment.

found that the relaxation theory is a good description of the response of 2.3-cm wind-generated waves to straining and that the relaxation rate is about twice the initial growth rate discussed previously [*Keller et al.*, 1974]. Finally, the notation used in this paper is listed in Table 1.

2. WAVE TANK AND INSTRUMENTATION

The two-scale scattering measurements reported here were made by the authors at the wave tank facility of the University of Florida, Gainesville. The wave tank is described by *Lai and Shemdin* [1971]. The tank, which is 91.5 cm wide, was operated with a water channel depth of 91.5 cm and a wind tunnel height of 91.5 cm.

Seven meters of roof section was removed to make way for the antenna. Wind profile measurements were made at the scattering site and the wind field is described in this paper by the air friction velocity, u^*, obtained from those profiles. Comparison of u^* with nominal wind tunnel speeds and oceanic winds is given by *Duncan et al.* [1974]. The maximum windspeed used here corresponds to a wind of perhaps 12–15 m sec^{-1} on the ocean. The tank was equipped with an overflow standpipe for the removal of surface films. We obtained results for scattering cross sections at low air friction velocities ($u^* \sim 10$ cm sec^{-1}) comparable to those obtained in another tank [*Duncan et al.*, 1974] where we know the removal of surface films was satisfactory. As the cross section at low winds is quite sensitive to the presence of surface films we believe the overflow standpipe arrangement was probably adequate to remove these films.

TABLE 1. List of symbols.

$a(\mathbf{k})$, $f_1(\mathbf{k})$, $f_2(\mathbf{k})$, $h(\mathbf{k}_1)$, $n(\mathbf{k})$	perturbation of surface displacement spectrum
d	mean depth of water in wave tank
$e(t)$	linearly detected, rectified, received signal
$f(t)$	random (wind-generated) constituent of $e(t)$
g	scattering function (equation 8)
$\mathbf{k}$, k	surface wave vector and wave number
k_x	component of wave number in x direction
k_0	microwave number
m	theoretical power modulation index (equation 33)
p	modulation index of received signal (equation 2)
r	measured peak-peak modulation of $R(\tau)$, (Figure 2)
t	time
$u(t)$	periodic constituent of $e(t)$
u^*	air friction velocity
x	Cartesian coordinate along tank axis
A_f	two-way illuminated area of antenna beam
A_i	illuminated area at surface (equation 7)
B	straining function (equation 30)
C	phase speed of plunger-generated wave
C_g, C_g^0	group speed of wind-generated wave with and without plunger-generated wave
C_0	phase speed of wind-generated wave in absence of plunger-generated wave
D	straining function (equation 31)
F, F_0	wind-wave surface displacement spectrum
G	scattering function (equation 11)
H	wave-wave interaction functional
I^0	equilibrium wave-wave interaction operator
K	plunger-generated wave number
M, M_u, M_d	measured fractional modulations (equation 5)
P	received power
P_0	received power in absence of plunger
$R(\tau)$	correlation function of $e(t)$
R_0	$R(o)$
S	plunger-generated wave slope
T	tilting function (equation 29)
T_a	averaging time
U	horizontal component of orbital velocity of plunger-generated wave
U_0	modulus of U
β	wind-generated wave growth rate
β_r	wind-generated wave relaxation rate
γ	straining constant
ϵ	statistical error
θ, θ'	depression angles (Figure 1)
σ^0	scattering cross section per unit area
τ	time lag
φ, φ'	phase angles
ω	radian frequency of wind-generated wave
Ω	radian frequency of plunger-generated wave

The antenna was a 30.5-cm diameter parabola focussed at the mean static water surface. The use of such antennas for scattering measurements is discussed by *Duncan et al.* [1974]. All measurements were made with vertical polarization, i.e., electric field in the plane of incidence. The depression angle was 45° and both upwind- and downwind-looking antenna orientations were used as shown in Figure 1. All measurements were made at 9.375 GHz. The microwave system was a coherent CW system similar to that used in our previous work [*Duncan et al.*, 1974; *Wright*, 1966], which utilizes a 400-Hz offset. That is, stationary scatterers appear at a frequency 400 Hz removed from the transmitted frequency. The coherent, i.e., Doppler, information is not an essential part of the results reported here, however. The system utilizes linear detection and the received signal was recorded on an analog tape recorder with a nominal dynamic range of 38 db. The signal, which is thus proportional to the square root of the received power, was subsequently rectified, filtered to remove components above 30 Hz, and autocorrelated with a Federal Scientific Corporation Model UL 202C correlator. If $e(t)$ is the received signal the unnormalized correlation function is denoted $R(\tau)$,

$$R(\tau) = (1/T_a) \int_0^{T_a} e(t)e(t + \tau)\, dt \tag{1}$$

The averaging time, T_a, was six minutes. Sample correlation functions are shown in Figure 2, left. It is evident that the received signal is divisible into components of different time scale and that the slower component is periodic, i.e.,

$$e(t) = f(t) + p\bar{f}u(t) \tag{2}$$

where $u(t)$ is periodic and $\bar{f}$ is the average over the time T. We define

$$R_0 \equiv \overline{f^2}(t) \tag{3}$$

If $u(t) = \cos(\Omega t)$

$$R(\tau) = (1/T_a) \int_0^{T_a} f(t)f(t + \tau)\, dt + (p^2/2)(\bar{f})^2 \cos(\Omega\tau) \tag{4}$$

The measured peak-to-peak modulation amplitude, r (Figure 2, left, IV) is then $r = p^2(\bar{f})^2$ and we define a functional modulation M

$$M \equiv r/R_0 \tag{5}$$

Wave height records were made simultaneously with the microwave records using capacitance type wave probes placed approximately 1.5 m from the spot illuminated by the antenna. Spectra were obtained from these records by analyzing in real time with a Federal Scientific Corporation Model UA-500 spectrum analyzer. Sample spectra are shown in Figure 2, right. Note that high pass filtering was used to reduce the fundamental plunger-generated wave spectral amplitude in order to keep the total spectral amplitude within the dynamic range of the analyzer. Approximately 4–6 db should be added to .575-Hz peaks in Figure 2, right, in comparing them with the higher harmonics and the wind wave system. Note also that for the spectrum in Figure 2 (right, IV) the noise level is, in effect, 10 db higher than for the other three spectra. We did not attempt to determine the frequency response of the capacitance probes as only qualitative use is made of the wind wave spectra in this report. It is manifest from Figure 2 (right) that they respond well at 5 Hz but they are probably losing response at 10 Hz. For the purpose of measuring the height of the plunger-generated waves, the capacitance probes were calibrated statically with each day's runs and the mean-square wave height was obtained by autocorrelation. As the plunger-generated waves are essentially periodic they are designated by their amplitude.

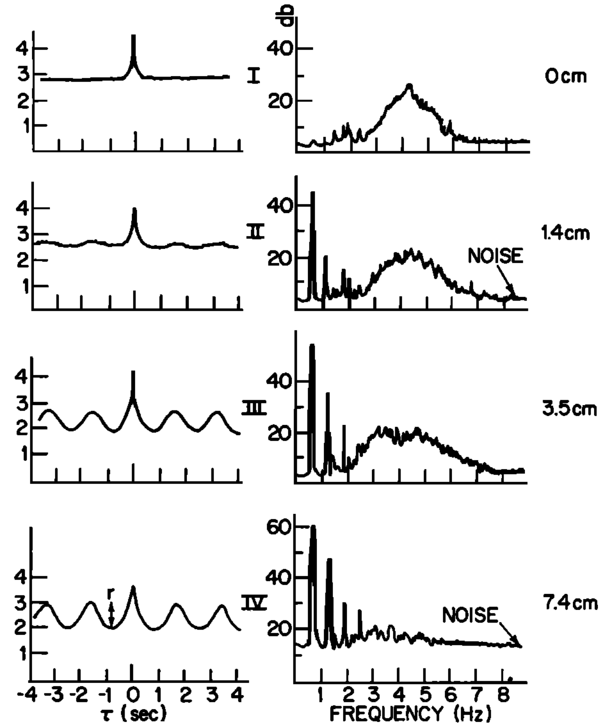

Fig. 2. Autocorrelation functions of the microwave return (left) and wind-wave spectra (right) for various wave amplitudes at $u^* = 16.5$ cm sec^{-1}.

3. TWO-SCALE SCATTERING

The small-scale waves of the two-scale wave system were generated by the wind and all measurements were made at a fetch of 8 m. The large-scale wave was a nearly monochromatic plunger-generated wave of controllable amplitude and frequency. However, all the measurements reported here were made at a frequency of 0.575 Hz. At this frequency the wave crests were nearly perpendicular to the wave tank axis. As the scattering on vertical polarization is insensitive to crosswind tilts in any case, these latter may be safely neglected in computing the backscattered power.

Provided the scatterers are decorrelated in a distance small compared to the large wavelength (which is 4.20 m for a 0.575-Hz wave) the backscattered power, P, is

$$P = \sigma^0 A_i \quad (6)$$

where σ^0 is the scattering cross section per unit surface area and A_i is the two-way illuminated area as defined by *Wright and Keller* [1971]. The area, A_f, at the focus, and in a plane perpendicular to the antenna axis was very nearly circular and of diameter 12 cm. At the large wave surface this becomes

$$A_i = A_f/\sin\theta' \quad (7)$$

The cross section in first-order scattering is given, e.g., by *Wright* [1968]:

$$\sigma^0 = 16\pi k_0^4 gg^* F(2k_0\cos\theta', 0, U) \quad (8)$$

The function g depends on the local depression angle and is also given by *Wright* [1968]. The local Bragg wave number is $2k_0\cos\theta'$. In the absence of a large-scale wave it has the value 2.72 cm^{-1} at 45° and 9.375 GHz. The power spectral amplitude of surface displacements of the small scale wave system is $F(k_x, k_y, U)$ where x and y are measured parallel and perpendicular to the tank axis. As will be seen later, it is convenient to use the horizontal component of orbital velocity, $U(x, t)$, to describe the large wave.

$$U(x, t) = U_0 e^{i(Kx-\Omega t)} \quad (9)$$

and the dependence of the spectral amplitude on x and t is contained implicitly in $U(x, t)$. The symbols K and Ω represent the wave number and angular frequency respectively of the large-scale wave. To first order in large wave slope the local slope is given by

$$S = j(U/C)\tanh(Kd)$$

where C is the phase speed and d the water depth. If P_0 is the mean backscattered power in the absence of any wave, the fractional change in backscattered power, $\Delta P/P_0$, due to tilting can be obtained to first order from the first term of a Taylor series expansion about $\theta' = \theta$:

$$\Delta P/P_0 = \pm S[(1/G)(dG/d\theta) - \tan\theta(k_x/F_0)\,\partial F_0/\partial k_x] \quad (10)$$

where

$$F_0 \equiv F(k_x, k_y, 0)$$

and

$$G \equiv gg^*/\sin\theta \quad (11)$$

The positive sign in (10) is applicable to the upwind antenna orientation and the negative sign to the downwind orientation.

4. STRAINING OF WIND-GENERATED WAVES

The straining of small waves by the horizontal component of orbital motion of larger waves is a well-known phenomenon [e.g., *Phillips,* 1966] but existing theories omit the wind- and wave-wave interactions. These cannot be ignored in the case of short gravity-capillary waves since these tend to exist in a steady state brought about, in large measure, by the counter action of these processes. The traditional tool of statistical physics for dealing with perturbations of such steady states is the Boltzmann transport equation, also referred to as the radiative transfer equation. For the case at hand, this equation is

$$\partial F/\partial t + C_g\,\partial F/\partial x - (\partial\omega/\partial x)\,\partial F/\partial k_x = \beta F - \gamma(k)(\partial U/\partial x)F + H(F, k) \quad (12)$$

In this equation, x and k_x are independent variables. They are, in fact, the Hamiltonian coordinate and momentum for wave packet trajectories in the upwind-downwind direction. That is

$$dx/dt = \partial\omega/\partial k_x \equiv C_g$$

$$dk_x/dt = -\partial\omega/\partial x$$

The angular frequency $\omega(k, x, t)$ can be computed as the eigenvalue of a local boundary value problem for the propagation of small surface displacements. That is, to first order in U_0/C,

$$\omega(k, x, t) = k_x U(x, t) + kC_0 \quad (13)$$

For irrotational waves

$$C_0 = [(g - \Omega U)/k + Sk]^{1/2} \quad (14)$$

where g is the acceleration of gravity and S the ratio of surface tension to water density. Thus $\partial\omega/\partial x$ is given by

$$\partial\omega/\partial x = k_x(1 - \Omega/2kC_0)\,\partial U/\partial x \qquad (15)$$

For the Bragg wavelength, $k = 2k_0 \cos\theta$, occurring in the measurements reported here, $kC_0 \sim 2\pi \times 10$ sec^{-1} so that the term $\Omega/kC_0 \simeq 2 \times 10^{-2}$. We will henceforth neglect this term though its inclusion in the final result would be straightforward.

The first term on the right-hand side represents the input from the wind. The second term has come to be called the "radiation stress" [*Longuet-Higgins and Stewart*, 1964], but in a paper dealing with the interaction of electromagnetic and water waves this terminology does not seem particularly clarifying and is herewith abandoned. The term may be thought of simply as a local growth or decay rate induced by straining just as, in *Miles*' [1957] theory of wave generation, β is a growth or decay rate induced by shear. The value of $\gamma(k)$ for irrotational waves calculated from that given by *Longuet-Higgins and Stewart* [1964] is

$$\gamma(k) = [1 + 3(k/k_m)^2]/2[1 + (k/k_m)^2] + 1 \qquad (16)$$

where $k_m = g/S$. It should be noted that short wavelength wind-generated waves are not really irrotational since they evolve from the wind drift [*Wright and Keller*, 1971; *Keller et al.*, 1974]. Thus (16) as well as (13) are only approximations valid for vanishing winds. We believe that these approximations are probably not crucial in the present context but this assumption requires critical reexamination in the future. Finally, $H(F, k)$ is a functional into which we lump nonlinear dissipative interactions about which we have no precise knowledge together with the better understood conservative, resonant wave-wave interactions. These last occur at second order for short gravity-capillary waves and have been given by *Valenzuela and Laing* [1972].

We now rewrite (12) in the frame moving at the phase speed of the large wave and expand the small-wave spectrum in a perturbation series

$$F = F_0 + (U_0/C)f_1 + (U_0/C)^2 f_2 + \cdots \qquad (17)$$

For convenience we give f_1 in terms of its components with respect to $U(x)$:

$$f_1 \equiv [h(\mathbf{k}) + jn(\mathbf{k})]e^{iKx} \qquad (18)$$

It is necessary to assume that F_0 satisfies the zeroth-order equation obtained from inserting (17) into (12) even though we do not in fact know $H(F, \mathbf{K})$ precisely, and the calculation of $F_0(k)$ would be a very difficult task in any event. We further assume that $H(F, \mathbf{k})$ may be expanded about the equilibrium state in the form

$$H \rightarrow H^0 + \int I^0(F_0, \mathbf{k}, \mathbf{k}')f_1(\mathbf{k}')\,d\mathbf{k}' + \cdots$$

Then:

$$(1 - C_g^0/C)\Omega n(\mathbf{k}) - \beta h(\mathbf{k}) - \int I^0(F_0, \mathbf{k}, \mathbf{k}')h(\mathbf{k}')\,d\mathbf{k}' = 0 \qquad (19)$$

$$-(1 - C_g^0/C)\Omega h(\mathbf{k}) - \beta n(\mathbf{k}) - \int I^0(F_0, \mathbf{k}, \mathbf{k}')n(\mathbf{k}')\,d\mathbf{k}' = (k_x\,\partial F_0/\partial k_x - \gamma F_0)\Omega \qquad (20)$$

We cannot evaluate I^0. We include it to motivate the next step which is the introduction of the relaxation time approximation. Suppose, then, that we perturb (12) in the absence of any straining current. That is, we make a small perturbation, f, of the equilibrium spectrum which we assume to have negligible spatial variation. Then, with the same type of approximation as above we obtain

$$\partial f(\mathbf{k}, t)/\partial t = \beta f(\mathbf{k}, t) + \int I^0(F_0, \mathbf{k}, \mathbf{k}')f(\mathbf{k}', t)\,d\mathbf{k}' \qquad (21)$$

This is a first-order integro-differential equation with solutions of the form

$$f(\mathbf{k}, t) \sim a(\mathbf{k})e^{-\beta_r t} \qquad (22)$$

so that (21) becomes

$$\int I^0(F_0, \mathbf{k}, \mathbf{k}')a(k')\,dk' = -(\beta + \beta_r)a(\mathbf{k}) \qquad (23)$$

The problem is thus reduced to that of finding the eigenvalues and eigenfunctions of the equilibrium operator I^0. It happens in many problems in statistical physics that I^0 is nearly diagonal. In the present case this would mean that in perturbations from equilibrium the original waves are essentially uncoupled. There is no obvious *a priori* reason why this should be the case. Its assumption is the relaxation time approximation:

$$\int I^0(F_0, \mathbf{k}, \mathbf{k}')f_1(\mathbf{k}')\,d\mathbf{k}' \equiv -(\beta + \beta_r)f_1(\mathbf{k}) \qquad (24)$$

Note that this approximation may be valid for some values of k but not for others. Its justification rests with comparison with experiment which is carried out in section 5.

With this assumption (19) and (20) reduce to simple algebraic equations with the solution

$$h(\mathbf{k})/F_0 = -\{[(1 - C_g^0/C)\Omega^2/\beta_r^2] \div [1 + (1 - C_g^0/C)^2\Omega^2/\beta_r^2]\} \cdot [(k_x/F_0)\,\partial F_0/\partial k_x - \gamma] \tag{25}$$

$$n(\mathbf{k})/F_0 = \{(\Omega/\beta_r)/[1 + (1 - C_g^0/C)^2\Omega^2/\beta_r^2]\} \cdot [(k_x/F_0)\,\partial F_0/\partial k_x - \gamma] \tag{26}$$

The response of the equilibrium wind wave system to harmonic strains of moderate amplitude is thus predicted to be a simple relaxation. At sufficiently low winds we expect that $\Omega/\beta_r \gg 1$ so that, when $\partial F_0/\partial k_x$ is negative, the response is in phase with the straining current. As the wind increases and Ω/β_r becomes less than unity, the phase of the response approaches that of the negative of the gradient of the straining current. At very high winds, the response vanishes. When $C = C_g^0$, (25) and (26) give meaningful results provided $\beta_r \neq 0$. If $\beta_r = 0$, and also $C = C_g^0$, then there is no steady-state solution. In identifying $h(k)$ and $n(k)$ as the components in phase and out of phase with respect to the straining current we have implicitly assumed β_r to be real. This need not necessarily be the case. In fact, insofar as observed overshoot phenomena represent an oscillatory approach to equilibrium, β_r may indeed be complex. Finally, in first-order Bragg scattering, and to first order in U_0/C

$$(\Delta P/P_0)_{\mathrm{strain}} = [h(k)/F_0 + j\,n(k)/F_0]\,U/C \tag{27}$$

5. MEASURED AND THEORETICAL MODULATIONS

At first order in U_0/C the tilting and straining effects simply add, i.e.,

$$\Delta P/P_0 = (\Delta P/P_0)_{\mathrm{tilt}} + (\Delta P/P_0)_{\mathrm{strain}} \tag{28}$$

Let us write:

$$(\Delta P/P_0)_{\mathrm{tilt}} = \pm jTU/C$$

and

$$(\Delta P/P_0)_{\mathrm{strain}} = (B + jD)\,U/C$$

where, from (10) and at $\theta = 45°$

$$T \equiv (\tanh Kd)[1/G(dG/d\theta) - (k_x/F_0)(\partial F_0/\partial k_x)] \tag{29}$$

and

$$B \equiv h/F_0 \tag{30}$$

$$D \equiv n/F_0 \tag{31}$$

Then

$$P = P_0[1 + m\cos(\Omega t + \varphi)] \tag{32}$$

where

$$m \equiv (B^2 + D^2 + T^2 \pm 2DT)^{1/2}(U_0/C) \tag{33}$$

and

$$\tan\varphi \equiv (D \pm T)/B \tag{34}$$

Again, the positive and negative signs in (34) refer to upwind- and downwind-looking antenna orientations respectively.

We may think of the received power given by (6) and (8) or (28) as having been obtained from an average over an ensemble, the members of which are exactly one plunger-generated wave period in length and synchronized. Such an average is sometimes called a phase average. Now recall that $e(t)$ is the square root of the received power. The instantaneous power at a given phase, $\varphi' = \Omega t + \varphi$, of the periodic large wave is then $e^2(t)$ and from (2),

$$e^2(t) = f^2 + 2pf(t)\bar{f}u(\varphi') + p^2u^2(\varphi') \tag{35}$$

At first order in U_0/C it is reasonable to assume that phase averages (denoted by $\langle\ \rangle$) and time averages are identical, so that, to first order in U_0/C,

$$P = \langle e^2\rangle = \overline{f^2} + 2p(\bar{f})^2u(\varphi') \tag{36}$$

Finally, comparison with (32) gives, to first order in U_0/C,

$$2p(\bar{f})^2 = mP_0 = m\overline{f^2} \tag{37}$$

Thus, to first order in U_0/C the measured fractional modulation, M, is related to the calculated power modulation index, m, by

$$M = (m^2/4)[\overline{f^2}/(\bar{f})^2] = (m^2/4)[R_0^2/(\bar{f})^2] \tag{38}$$

We found, from all the measurements on 0.575-Hz waves reported here, that $R_0/(\bar{f})^2 = 1.4 \pm .02$. Thus

$$M = .35m^2 \tag{39}$$

The statistical error in these fractional modulations can be estimated from the variance in $f(t)$, $[R_0/(\bar{f})^2 - 1]$, and the decorrelation time of the random, i.e., wind-generated portion of $e(t)$. The latter, estimated from the width of the spikey portion of the autocorrelation function near $\tau = 0$ was clearly of the order of the period of the dominant wind-generated wave. This was 1/3 sec or less. In a six-min record there are of the order of 10^3 independent samples of $f(t)$ and the error, ϵ, in $\bar{f}$ is

$$\epsilon \sim \{(10^{-3})[R_0/(\bar{f})^2 - 1]\}^{1/2} \simeq .02$$

This error estimate is reasonably consistent with our observation that fractional modulations of .02 were readily measurable but those less than .01 were not.

Values of M_u and M_d, the fractional modulations measured looking upwind and downwind respectively are given in Figure 3 as a function of u_a*. The 0.575-Hz plunger-generated wave was of nearly constant amplitude, 5.5 cm, for both upwind and downwind measurements. It is evident that the modulations are quite different for the two orientations. Furthermore, the modulation looking downwind becomes very small as is predicted by (33) if the relaxation time becomes equal to the angular frequency of the plunger-generated wave within the wind-speed range under investigation. Comparison between theory and measurements is best carried out in terms of the quantities $M_u \pm M_d$.

From (33), (38), and (39) these are

$$M_u + M_d = 0.7(B^2 + D^2 + T^2) \quad (40)$$

$$M_u - M_d = 1.4DT \quad (41)$$

Since T is independent of the wind $M_u - M_d$ should thus be proportional to D and have a maximum at approximately the wind where $\beta_r = \Omega$. This occurs at $u^* = 20$ cm sec^{-1} (Figure 5) and gives $\beta_r = 3.6$ sec^{-1} at that wind. This is about twice the initial temporal growth rate for 2.3-cm waves at $u^* = 20$ cm sec^{-1} which we also measured. In order to compare theoretical and measured modulation magnitudes we

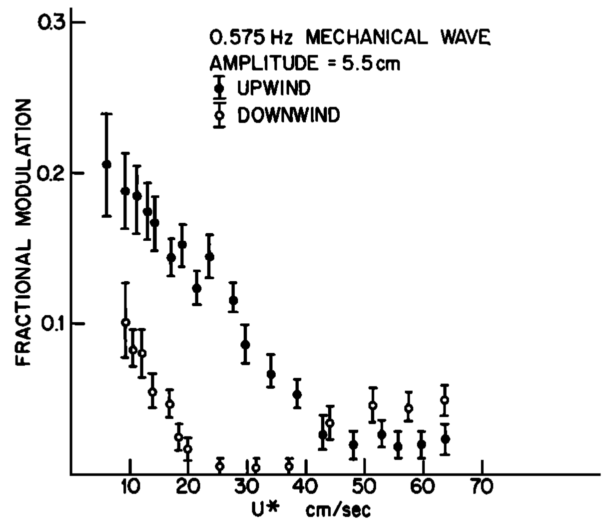

Fig. 3. Fractional modulation vs. air friction velocity for 0.575-Hz wave, $U_0/C = 0.091$; solid circles, upwind; open circles, downwind.

use values of $(k/F_0)/\partial F_0/\partial k$ obtained from photometric measurements of directional slope spectra at a fetch of 3 m given by *Wright and Keller* [1971]. This quantity, together with the appropriate combinations with $\gamma(k)$ and $(1/G)dG/d\theta$, are given in Table 2. The comparison is shown as a function of plunger wave amplitude for two wind speeds in Figure 4. The measured modulations agree well with the calculated ones but appear to saturate for $U_0/C > 0.08$. If we simply normalize the value of $M_u - M_d$ to the measured value at the wind speed of maximum $M_u - M_d$ and take β_r to be twice the measured growth rates at all winds, then the calculated curves are nonetheless an excellent fit to the data of Figure 3 (for which $U_0/C = 0.091$) for air friction velocities less than about 40 cm sec^{-1} (Figure 5). At higher winds,

TABLE 2. Spectral parameters.

u^* (cm sec^{-1})	$-\left(\frac{k_x}{F_0}\frac{\partial F_0}{\partial k_x}\right)$	$-\left(\frac{k_x}{F_0}\frac{\partial F_0}{\partial k_x} - \gamma\right)$	$-\left(\frac{k_x}{F_0}\frac{\partial F_0}{\partial k_x} - \frac{1}{G}\frac{dG}{d\theta}\right)$
10	7.7	9.6	5.9
15	7.2	9.2	5.5
20	6.9	8.8	5.1
25	6.5	8.4	4.7
30	6.1	8.0	4.4
35	5.7	7.6	3.9
40	5.2	7.1	2.3
50	4.5	6.4	2.7
60	3.7	5.6	1.9

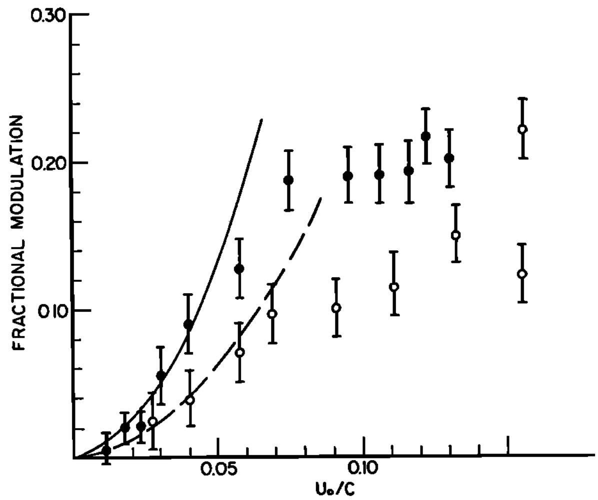

Fig. 4. Comparison of theoretical and measured fractional modulations looking upwind vs. orbital velocity of 0.575-Hz waves. Solid data points and solid line are for $u^* = 16.5$ cm sec^{-1}. Open data points and dashed line are for $u^* = 30$ cm sec^{-1}.

there is definitely another phenomenon present not accounted for by the relaxation theory.

We also measured the phase of the modulated return by cross correlation with the output of the capacitance probe. The phase angle by which the modulated return leads the crest of the plunger-generated wave is shown in Figure 6 for the same wind and wave conditions as those of Figure 4. It is evident that this phase is relatively independent of wave amplitude though there appears to be a significant increase of phase at the largest wave amplitudes. Values of phase calculated from (34) are also shown on Figure 6. These are about 20° greater than the measured phases at both wind speeds. The error in the calculated phases due to uncertainty in antenna boresighting and wave probe position should not exceed 5°. The origin of the additional discrepancy is unknown.

6. DISCUSSION

Several factors show that the first-order (in U_0/C) straining theory is not entirely adequate. The apparent saturation of the fractional modulation with increasing wave slope shown in Figure 4 has already been remarked upon. A second indication is the diminution of the wind-wave spectrum with increasing plunger-generated wave amplitude shown in Figure 2, right. Some of this diminution is simply the result of spectral broadening due to advection of the wind-wave system by the orbital motion of the plunger-generated waves. At the largest wave amplitude, however, there does appear to be a real decrease in the surface displacement of the wind-wave system due, perhaps, to nonlinear straining. Iteration of the perturbation procedure used in section 4 is not entirely straightforward because one must make further assumptions about the expansion of H at second order. If we ignore this and simply carry through an iteration to second order in U_0/C utilizing the relaxation time approximation we do find that there is a deletion of mean spectral amplitude near the peak in $F_0(k)$. However, to do the entire problem, including scattering, correctly at second order we must take nonlinear tilting into account as well as the fact that the scattering contributions from tilt and strain are no longer simply additive. This much more complex situation is left to a future work.

There is, however, one interesting inference concerning higher-order scattering to be drawn from the relative insensitivity of the mean backscattered power to wave amplitude compared to the diminution of the peak spectral amplitude by the largest plunger-generated wave, as seen in Figure 2. The point is that

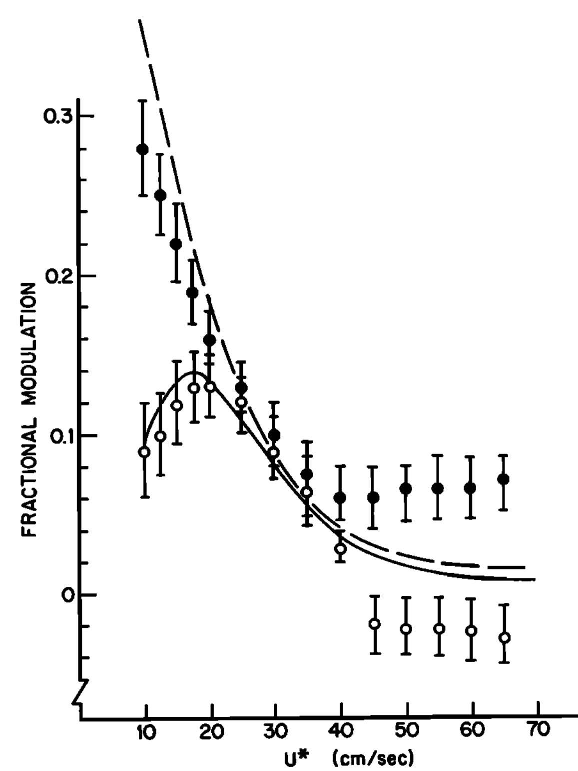

Fig. 5. Comparison of measured modulations with linear straining and tilting theory. Solid circles: $(M_u + M_d)$; open circles: $(M_u - M_d)$; 0.575-Hz wave; $U_0/C = 0.091$.

in second-order scattering, say, the scattering cross section will contain a term proportional roughly to the product of the Bragg wave and dominant wind-wave spectral amplitudes. If the dominant wind wave, in this case about 10 cm in wavelength, decreases in amplitude one would expect a corresponding decrease in scattering cross section if higher-order scattering were significant. Little decrease is observed.

Finally, as to the minor disparity between measured and theoretical modulation amplitudes, we note first of all that these amplitudes are roughly proportional to the square of $(k_x/F_0)\partial F_0/\partial k_x$ and so are sensitive to the value used. The values are taken from measurements at 3-m fetch whereas the modulation measurements were made at 8 m. We previously pointed out that the short wavelength wind waves evolve from the wind drift so that both $\gamma(k)$ and $\partial\omega/\partial x$ may be different than assumed.

7. CONCLUSIONS

The response of 2.3-cm wind-generated waves to modulation by 0.575-Hz (4.20-m wavelength) waves of moderate amplitude is essentially a relaxation characterized by a single relaxation time for air friction velocities less than about 40 cm sec^{-1}. The relaxation rate is about twice the wind-induced growth rate. At higher winds and larger wave amplitudes the linear theory given here is no longer adequate. Nonetheless, the modulation of wind-wave systems by mechanically generated waves is a useful tool for studying wave-wave interactions among short gravity-capillary waves through determination of relaxation times. For this purpose, values of U_0/C should not exceed about 0.1.

Acknowledgments. It is a pleasure to acknowledge the encouragement and cooperation of O. Shemdin, without whom this experiment could not have been accomplished. This work was performed, in part, under contract NA-756-73 with the National Environmental Satellite Service.

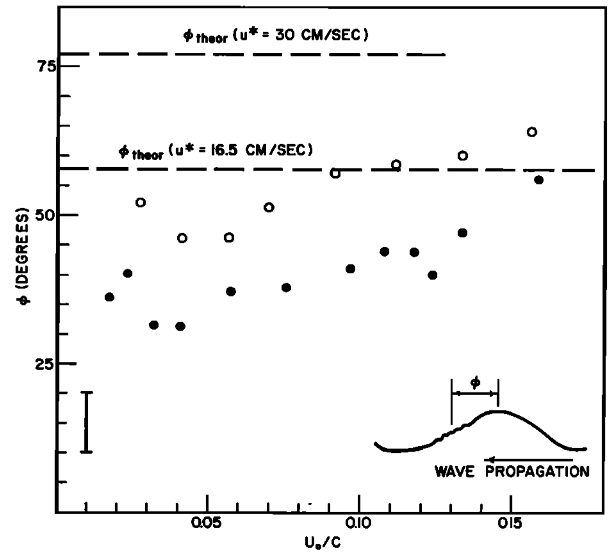

Fig. 6. The phase angle by which the modulated microwave return leads the wave crest as a function of orbital velocity. Solid circles: $u^* = 16.5$ cm sec^{-1}; open circles: $u^* = 30$ cm sec^{-1}.

REFERENCES

Duncan, J. R., W. C. Keller, and J. W. Wright (1974), Fetch and wind speed dependence of Doppler spectra, *Radio Sci.*, *9*, 809–819.

Guinard, N. W., and J. C. Daley (1970), An experimental study of a sea clutter model, *Proc. IEEE*, *58*, 543–550.

Keller, W. L., T. R. Larson, and J. W. Wright (1974), Mean speeds of wind waves at short fetch, *Radio Sci.*, *9*, 1091–1100.

Lai, R. J., and O. H. Shemdin (1971), Laboratory investigation of air turbulence above simple water waves, *J. Geophys. Res.*, *76*, 7334–7350.

Longuet-Higgins, M. S., and R. W. Stewart (1964), Radiation stresses in water waves: A physical discussion with applications, *Deep-Sea Res.*, *11*, 529–562.

Miles, J. W. (1957), On the generation of surface waves by shear flows, *J. Fluid Mech.*, *3*, 185–204.

Phillips, O. M. (1966), *The Dynamics of the Upper Ocean*, pp. 56–63, Cambridge University Press, London.

Valenzuela, G. R., and M. B. Laing (1972), Linear energy transfer in gravity-capillary wave spectra, with applications, *J. Fluid Mech.*, *54*, 508–520.

Wright, J. W. (1966), Backscattering from capillary waves with application to sea clutter, *IEEE Trans. Antennas Propagat.*, *14*, 749–754.

Wright, J. W. (1968), A new model for sea clutter, *IEEE Trans. Antennas Propagat.*, *16*, 217–223.

Wright, J. W., and W. C. Keller (1971), Doppler spectra in microwave scattering from wind waves, *Phys. Fluids*, *14*, 466–474.